Genome-wide screen for deficiencies modifying *Cyclin G*-induced developmental instability in *Drosophila melanogaster*

Valérie Ribeiro[1], Marco Da Costa[1], Delphine Dardalhon-Cuménal [1], Camille A. Dupont[1], Jean-Michel Gibert[1], Emmanuèle Mouchel-Vielh[1], Hélène Thomassin[1], Neel B. Randsholt[1], Vincent Debat[3]* and Frédérique Peronnet[1]*

[1] Sorbonne Université, CNRS, Inserm, Développement Adaptation et Vieillissement, Dev2A, F75005 Paris, France

[2] Sorbonne Université, CNRS, Inserm, Institut de Biologie Paris-Seine, IBPS, F75005 Paris, France

[3] Institut de Systématique, Evolution, Biodiversité (ISYEB), Muséum national d'Histoire naturelle, CNRS, Sorbonne Université, EPHE, Université des Antilles CP 50, 57 rue Cuvier, 75005 Paris, France

Valerie.Ribeiro@sorbonne-universite.fr
marco.da_costa@sorbonne-universite.fr
delphine.cumenal@sorbonne-universite.fr
camille.a.dupont@gmail.com
Jean-Michel.Gibert@sorbonne-universite.fr
Emmanuele.Mouchel@sorbonne-universite.fr
helene.thomassin-bourrel@sorbonne-universite.fr
neelbodil@gmail.com

*** Correspondence:**

Co-last and co-corresponding Author

frederique.peronnet@sorbonne-universite.fr

vincent.debat@mnhn.fr

Running title: Developmental stability

Keywords: Developmental instability, Drosophila, Fluctuating asymmetry (FA), Cyclin G, Genetic screen

ABSTRACT

Despite long-lasting interest and research efforts, the genetic bases of developmental stability – the robustness to developmental noise – and its most commonly used estimator, fluctuating asymmetry (FA), remain poorly understood. The *Drosophila melanogaster Cyclin G* gene (*CycG*) encodes a transcriptional cyclin that regulates growth and the cell cycle. Over-expression of a potentially more stable isoform of the protein (deleted of a PEST-rich domain, hereafter called CycG$^{\Delta P}$) induces extreme wing size and shape FA (*i.e.* high developmental noise), indicating a major disruption of developmental stability. Previous attempts to identify the genetic bases of FA have been impeded by the constitutively low level of developmental noise, limiting the power to detect any effect. Here, we leverage the extreme developmental instability induced by overexpression of *CycG*$^{\Delta P}$ to explore the genetic bases of FA: we perform a genome-wide screen for deficiencies that enhance or reduce *CycG*$^{\Delta P}$-induced wing FA. 499 deficiencies uncovering 90% of the euchromatic genome were combined with a recombinant chromosome expressing *CycG*$^{\Delta P}$. We identified 13 and 16 deficiencies that respectively enhance and decrease FA. Analysis of mutants for some genes located in these deficiencies shows that Cyclin G ensures homogeneous growth of organs in synergy with the major morphogens of the wing, Dpp and Wg, as well as the Hippo and InR/TOR pathways. They also reveal that *CycG*$^{\Delta P}$-induced FA involves Larp, a potential direct interactor of Cyclin G, that regulates translation at the mitochondrial membrane. This opens up new research perspectives for understanding developmental stability, suggesting a significant role for mitochondrial activity.

54 **INTRODUCTION**

55

56 Developmental noise results from the inherent variability of biological processes, that
57 operates independently of genetic or environmental factors (for a review on concepts see
58 (Debat and David 2002). Developmental stability refers to the buffering of developmental
59 noise. In bilaterians, as both sides are influenced by the same environmental conditions and
60 have the same genome, an estimate of developmental noise is provided by fluctuating
61 asymmetry (FA), the slight, random deviations from perfect symmetry in paired structures.
62 The genetic bases of developmental stability remain largely unknown. Investigation of
63 mandible size and shape FA in a population of mice has identified a few single-locus
64 Quantitative Loci Traits (QTLs) (Leamy et al. 2015). In *Drosophila*, the wings, which have a
65 highly stereotyped organisation, have been commonly used to measure FA (*e.g.* Breuker et
66 al. 2006; Takahashi, Okada, Teramura, et al. 2011; Gomez and Norry 2012; see Debat and
67 Peronnet 2013 for a review). Genome-wide deficiency mapping of regions responsible for
68 developmental noise has identified deficiencies associated with increased centroid size or
69 shape FA (Takahashi, Okada, Teramura, et al. 2011; Takahashi, Okada, and Teramura
70 2011). A few individual mutants have been reported to exhibit high FA, suggesting that they
71 may encode genes crucial for maintaining developmental stability. These include insertional
72 mutants for several members of the BMP signaling pathway (Debat et al. 2009), mutants for
73 the proapoptotic gene *hid* (Neto-Silva et al. 2009), mutants for the *Drosophila insulin-like*
74 *peptide 8* (*Dilp8*) gene and mutants for *Lgr3* that encodes its neuronal receptor (Colombani
75 et al. 2012; Garelli et al. 2012; Colombani et al. 2015; Garelli 2015), mutants for genes
76 encoding small Hsp proteins (Takahashi et al. 2010), mutant for the transcription factor Yorkie
77 (Srivastava et al. 2020) and mutants for the *Tsp1* gene, which encodes the trehalose-6-
78 synthase phosphate (Matsushita and Nishimura 2020). Strikingly, these genes are involved
79 in a wide range of biological processes — including growth, signaling, stress response, and
80 metabolism — indicating that developmental stability is unlikely to be controlled by a single
81 master regulatory mechanism. Instead, it appears to be a multifactorial trait arising from the
82 integration of multiple physiological pathways.

83 We have previously reported that the *Cyclin G* gene (*CycG*) of *Drosophila*
84 *melanogaster,* which encodes a transcriptional cyclin, is implicated in developmental noise
85 (Debat et al. 2011; Debat and Peronnet 2013). Indeed, overexpression of $CycG^{\Delta P}$, a modified
86 version of Cyclin G that lacks the C-terminal PEST domain and is therefore potentially more

87 stable, induces an unprecedented high level of size and shape FA (40-fold increase compared
88 to control). The strongly destabilized system induced by *CycG*$^{\Delta P}$ overexpression offers a
89 unique opportunity to investigate the genetic bases of developmental stability. In this study
90 we used *CycG*$^{\Delta P}$ overexpression to perform a genome-wide screen for deficiencies that
91 enhance or reduce *CycG*$^{\Delta P}$-induced wing size FA. 495 deficiencies uncovering about 90% of
92 the euchromatic genome were combined with a recombinant chromosome expressing
93 *CycG*$^{\Delta P}$.

94 Development robustness includes both developmental stability – *i.e.* the robustness to
95 developmental noise – and canalization – the robustness to genetic and environmental effects
96 (Debat and David 2002). As the relationship between these two components of robustness
97 has long been debated (see Klingenberg 2019 for a review), we also measured the variation
98 among individuals within genotypes as a measure of canalization, and tested its association
99 with FA.

100

101 **MATERIAL AND METHODS**

102

103 **Genetics**

104 Flies were raised in yeast-cornflour broth (yeast extract 75 g/L, cornflour 90 g/L, agar-
105 agar 10.7 g/L, methyl 4-hydroxybenzoate 5.5 g/L) at 25°C. Lines carrying deficiencies (*Df*)
106 were from the Bloomington deficiency kit which combines deficiencies from different sources
107 (BSC, Exelixis and DrosDel) (Cook et al. 2012) (Supplementary Table 1). The BSC
108 deficiencies numbered greater that 99 and the Exelixis deficiencies were generated in the
109 same isogenic background (BL-6326 stock) (Hoskins et al. 2001; Cook et al. 2012; Roote and
110 Russell 2012). The DrosDel deficiencies were generated in a different isogenic background
111 (BL-5905 stock) (Ryder et al. 2004). These stocks were used as negative controls for the
112 corresponding lines. The genetic backgrounds are referred to as w^{5905} or w^{6326}. For the other
113 59 lines, for which the genetic background is unknown, either w^{5905} or w^{6326} were used
114 interchangeably.

115 The mutant alleles used in this study are listed in Supplementary Table 2. The *da-*
116 *Gal4,UAS-CycG*$^{\Delta P}$ third chromosome, obtained by genetic recombination (Debat et al. 2011),
117 was used as a positive control. Due to high lethality and low fertility, this chromosome was
118 maintained against the *TM6c,Sb* balancer, in males, at 18°C.

119 In order to address the genetic interactions between *CycG* and each deficiency, 5
120 replicate crosses containing 6 deficiency or control females and 5 *da-Gal4*, *UAS-*
121 *CycG$^{\Delta P}$/TM6c,Sb* or *da-Gal4* males were performed. Series of experiments with up to 25
122 deficiencies were performed, each series including the appropriate positive and negative
123 controls. Care was taken to keep the crosses in standardized conditions: tubes used for a
124 given series were from the same batch, they were maintained at 25°C on the same incubator
125 floor, parents were transferred into new tubes each 48 h, three times, then discarded. The
126 offspring was counted and kept in 70 % ethanol. Thirty females of the desired genotype
127 (*Df/da-Gal4*, *UAS-CycG$^{\Delta P}$*, *+/da-Gal4*, *UAS-CycG$^{\Delta P}$*, *Df/da-Gal4* or *+/da-Gal4*) were
128 randomly sampled (Supplementary Figure 1).
129
130 **Measurements and statistical analysis**
131 The wings were mounted on slides and scanned as described in Debat et al. (2011).
132 The distance between landmarks 3 and 13 was used to estimate wing length (Supplementary
133 Figure 1). FA was analyzed following the recommendations of Palmer, A. R. and Strobeck,
134 C. (2003). As measurement error statistically behaves in a similar way as genuine FA (i.e.
135 non directional random variation), each measurement was taken twice and FA was estimated
136 using the FA10a index, as it allows to partition out measurement error from true FA (Palmer
137 & Strobeck 2003). Briefly, a two-way mixed model ANOVA was applied to the data,
138 considering "Individual" as a random effect and "side" as a fixed effect, repetitions being
139 included in the residuals of the model. FA10a was computed as the interaction "individual x
140 side" MS minus the residual MS, divided by the number of replicates (here two replicates).
141 FA10a is thus analogous to a variance and as such is expressed in squared units of length.
142 Differences in FA were then tested using standard F tests.
143 The nortest R package was used to test normality of the difference between left- and
144 right-wing size (Shapiro-Wilk and Lilliefors tests) as well as skewness and kurtosis. Indeed,
145 normality is a crucial aspect of FA distribution, as a lack thereof is often associated with
146 phenomena interfering with FA (*e.g.* bimodality might indicate antisymmetry; see Palmer 1994
147 and Palmer & Strobeck 2003 for details). The rare outliers that perturbated normality,
148 skewness (< -0.5 or > +0.5) or kurtosis (< -3 or > +3) were eliminated from the sample (see
149 number of individuals in Supplementary Table 3), as they were identified as obvious errors in
150 the measurements. When size varies among groups, differences in asymmetry might stem
151 from positive allometric effects (*i.e.* larger size genotypes might present larger asymmetries).

152 Results were thus checked for any size-dependence of FA. F-tests were performed to
153 compare FA of the assays to the one of the series internal controls (*Df*/*da-Gal4*, *UAS-CycG*$^{\Delta P}$
154 compared to +/*da-Gal4*, *UAS-CycG*$^{\Delta P}$, *Df/da-Gal4* compared to *+/da-Gal4*). Holm correction
155 was applied within each series to account for multiple testing. Inter-individual variance of wing
156 length represented the variance of the individual mean wing length in the same group.
157

158 **RESULTS**

159 **Genome-wide screen for deficiencies that modify *CycG*-induced fluctuating**
160 **asymmetry**

161 To scan the whole genome for modification of *CycG*$^{\Delta P}$-induced FA, we used a set of 499
162 deficiencies uncovering approximately 90% of the euchromatic genome (Supplementary
163 Table 1). Of these, 4 deficiencies were too weak to be crossed (Supplementary Table 1). A
164 primary screen was performed by crossing females of the remaining 499 deficiencies with *da-*
165 *Gal4*, *UAS-CycG*$^{\Delta P}$*/TM6c,Sb* males (Supplementary Figure 1). As the FA values varied from
166 experiment to experiment, a positive control (*w* females of the same genetic background
167 crossed with *da-Gal4*, *UAS-CycG*$^{\Delta P}$*/TM6c,Sb* males) and a negative control (*w* females of the
168 same genetic background crossed with *da-Gal4/TM6c,Sb* males) were systematically
169 included in each experimental series to serve as intrinsic standards. Of note, a number of
170 deficiencies (59 out of 499) were generated in an unknown genetic background (indicated as
171 *w* in Supplementary Figure 1). In these cases, the results may reflect not only the hemizygous
172 allelic effects revealed by the deficiencies but also potential influences of the genetic
173 background. Forty-one deficiencies were lethal or sub-lethal when combined with the *da-*
174 *Gal4*, *UAS-CycG*$^{\Delta P}$ chromosome, preventing FA analyses (Supplementary Table 1). Two
175 deficiencies produced damaged wings when combined with *da-Gal4*, *UAS-CycG*$^{\Delta P}$, rendered
176 them unmeasurable (Supplementary Table 1). A total of 16,200 fly wings were mounted and
177 analysed in this primary screen. Of the 452 deficiencies whose combination with *da-*
178 *Gal4*, *UAS-CycG*$^{\Delta P}$ produced viable flies with usable wings, most did not modify *CycG*$^{\Delta P}$-
179 induced FA (neutral deficiencies) (Supplementary Figure 2). However, 39 deficiencies and 21
180 significantly decreased or increased *CycG*$^{\Delta P}$-induced FA, respectively. We then performed a
181 secondary screen by crossing females of these 60 deficiencies with *da-Gal4*, *UAS-*
182 *CycG*$^{\Delta P}$*/TM6c,Sb* or *da-Gal4* males in order to replicate the primary screen while measuring
183 the FA of the deficiencies independently of *CycG*$^{\Delta P}$ overexpression. In addition, 8 neutral
184 deficiencies were randomly selected to confirm the absence of an effect. The results of this

185 secondary screen – a total of 4640 fly wings were mounted and analysed – are shown in
186 Supplementary Table 3. Of the 68 deficiencies tested, only three, *Df(2L)BSC17*,
187 *Df(1)BSC582*, and *Df(3L)BSC419*, increased FA when combined with *da-Gal4* in absence of
188 *CycG*$^{\Delta P}$ expression. None decreased it. Nevertheless, the increase was rather modest
189 compared to that observed in context of *CycG*$^{\Delta P}$ expression (FA fold-changes of 3.3, 3.4, and
190 4.8 when comparing *Df/+; +/da-Gal4* to *+/da-Gal4* of the same series, *versus* FA fold-changes
191 of 28.5, 73.4, and 73.4 when comparing *+/UAS-CyG*$^{\Delta P}$*,da-Gal4 to +/da-Gal4* of the same
192 series). Interestingly, *Df(3L)BSC419* partially overlaps *Df(3L)ED4978*, which has already
193 been shown to increase wing shape FA (Takahashi, Okada, Teramura, et al. 2011).

194 The absence of *CycG*$^{\Delta P}$-induced FA modification was verified for the 8 neutral
195 deficiencies. However, the secondary screen eliminated some deficiencies whose effect on
196 *CycG*$^{\Delta P}$-induced FA was no longer significant, probably due to the variability of the internal
197 control. Thus, the screen ended up with 29 modifier deficiencies: 16 that reproducibly
198 decreased *CycG*$^{\Delta P}$-induced FA and 13 that reproducibly enhanced it, further referred to as
199 decreasing and enhancing deficiencies, respectively (Table 1 and Figure 1). Surprisingly, the
200 13 enhancing deficiencies clustered on the second chromosome and the left arm of the third
201 chromosome whereas the 16 decreasing deficiencies clustered on the X chromosome and
202 the right arm of the third chromosome (Table 1). We did not observe any significant correlation
203 between the length of these deficiencies and the amplitude of their effect on *CycG*$^{\Delta P}$-induced
204 FA (Figure 2A). A comparison of the secondary screen with a previous screen covering
205 approximately 65% of the *Drosophila melanogaster* genome (Takahashi, Okada, Teramura,
206 et al. 2011) revealed that, among the 9 decreasing and 16 increasing deficiencies that are
207 shared, none showed any alteration in wing centroid size FA, highlighting the power of the
208 *CycG*$^{\Delta P}$ genetic background to detect developmental noise (Supplementary Table 4).

209 The mean wing size of all *Df; da-Gal4*, *UAS-CycG*$^{\Delta P}$ flies was smaller than that of *Df;*
210 *da-Gal4* flies, indicating that *CycG*$^{\Delta P}$ expression had a dominant effect on size reduction
211 (Figure 2B and Supplementary Figure 3). These differences in asymmetry were not due to a
212 size-dependent effect, as wing size was smaller (and not larger) in the most asymmetric
213 genotypes, and thus reflected genuine differences in developmental stability (Palmer, A. R.
214 and Strobeck, C. 2003).

215 Lastly, we observed a positive correlation between FA and inter-individual variance
216 mostly driven by a joint difference among broad categories of genotypes, *i.e.* deficiencies
217 alone, with low levels of both FA and individual variance, and high levels in the enhancing

218 deficiencies combined with *CycG*$^{\Delta}$, the decreasing deficiencies showing intermediate values
219 when combined to *CycG*$^{\Delta}$ (Figure 2C), As environmental conditions cannot be fully controlled
220 and individuals are not genetically perfectly identical due to potential segregating variation in
221 the parental lines, this inter-individual variance thus reflects minute genetic and environmental
222 differences, and indirectly, canalization (*e.g.* Klingenberg 2019). This positive correlation
223 between FA and inter-individual variance suggests that developmental stability and
224 canalization of *Drosophila* wing can be jointly affected by the combination of the deficiencies
225 and *CycG*$^{\Delta}$.

226 Taken together, these results confirmed that *CycG*$^{\Delta P}$ expression strongly perturbs
227 developmental stability. In addition, we identified 29 deficiencies among the 452 analysed
228 that enhanced or decreased *CycG*$^{\Delta P}$-induced FA and could thus contain genes important for
229 developmental stability. These genes could therefore be partners of *CycG* in the mechanisms
230 that maintain developmental stability.

231

232 **Identification of genes that modify *CycG*$^{\Delta P}$-induced fluctuating asymmetry**

233 We next set out to identify partners of *CycG* in developmental stability within these
234 deficiencies. Interestingly, *Df(3R)ED6361*, which uncovers *CycG*, reduced the FA induced by
235 *CycG*$^{\Delta P}$ expression, suggesting that expression of *CycG*$^{\Delta P}$ behaved as a dominant negative
236 mutant and that the deviation from symmetry it induced was dose-dependent. Taken together,
237 the enhancing deficiencies contained 736 genes (576 protein-coding genes and 160 non-
238 protein-coding genes), and the decreasing deficiencies 865 genes (715 protein-coding genes
239 and 150 non-protein-coding genes), making it impossible to test mutants of these genes
240 individually. To select which mutants to test, we focused on genes encoding direct protein
241 partners of Cyclin G or genes involved in the control of growth (Supplementary Table 2).

242 Although located in decreasing deficiencies (Supplementary Table 3), mutants or RNAi
243 lines for *Aladin* (Carvalhal et al. 2015), *CG9426* (FBgn0032485), *E5* (Dalton et al. 1989),
244 *eEF2* (Marygold et al. 2017), and *SAK* (Bettencourt-Dias et al. 2004) which encode direct
245 Cyclin G physical interactors, significantly increased *CycG*$^{\Delta P}$-induced FA (Figure 3). Other
246 genes, or combinations of genes, in these deficiencies may be responsible for the observed
247 effects. On the other hand, two RNAi lines for *larp*, which is located in a decreasing deficiency
248 (*Df(3R)BSC322*) and also encodes a direct Cyclin G physical interactor (11), significantly
249 reduced *CycG*$^{\Delta P}$-induced FA (Figure 3). Larp and Cyclin G may thus be direct partners in a
250 process important for developmental stability.

251 The Hippo signalling pathway plays a key role in controlling organ size (10). *Merlin*
252 (*Mer*), which encodes a positive regulator of this pathway that interacts directly with Cyclin G
253 (11), is located in the decreasing deficiency *Df(1)BSC871*. Additionally, *hippo* (*hpo*), which
254 encodes the kinase of the pathway, is located in *Df(2R)ED3728*, which increased *CycG*$^{\Delta P}$-
255 induced FA. This prompted us to investigate the impact of other members of the Hippo
256 pathway on *CycG*$^{\Delta P}$-induced FA. Mutants for *Mer, hpo, ft*, *exp*, *wts* and *ban*, significantly
257 increased it (Figure 4A). Furthermore, *Mer* inactivation also increased FA independently of
258 *CycG* deregulation (Figure 4A). These results suggest that the Hippo pathway plays a role in
259 developmental stability.
260 The *mTor* gene, which encodes the central member of another key regulator of growth
261 (Grewal 2009), the InsulinR/TOR signalling pathway (InR/TOR) belongs to a deficiency that
262 reduced *CycG*$^{\Delta P}$-induced FA [*Df(2L)BSC277*]. Furthermore, Cyclin G interacts directly with
263 three actors of this pathway: Akt1, PP2A and Wdb (Fischer et al. 2016; Oughtred et al. 2021).
264 We thus tested the effect of *mTor* and other members of the pathway for their effect on
265 *CycG*$^{\Delta P}$-induced FA. Most of these, particularly mutants for *Akt1*, *S6K*, *foxo*, *PTEN*, *mTor* and
266 *wdb*, increased *CycG*$^{\Delta P}$-induced FA. This suggests that the interaction between Cyclin G and
267 the InR/TOR pathway is crucial for developmental stability (Figure 4B).
268 Finally, two major morphogens of the wing, *dpp* and *wg* [for a review see (Tabata and
269 Takei 2004)], belonged to deficiencies that enhanced *CycG*$^{\Delta P}$-induced FA [*Df(2L)Exel7011*
270 and *Df(2L)BSC291*, respectively]. Mutants for both genes also increased *CycG*$^{\Delta P}$-induced
271 FA, indicating that we had identified at least one gene responsible for this effect within each
272 deficiency (Figure 4C).
273
274 **DISCUSSION**
275
276 In our efforts to identify deficiencies that modify *CycG*$^{\Delta P}$-induced FA, we found that 13
277 deficiencies out of 452 enhanced it (enhancing deficiencies) while 16 deficiencies decreased
278 it (decreasing deficiencies). Notably, these deficiencies were not evenly distributed across all
279 chromosomes. The decreasing deficiencies were enriched on chromosomes X and 3R,
280 whereas the enhancing deficiencies were concentrated on chromosomes 2 and 3L. This
281 pattern suggests that chromosomes 2 and 3L may have a general positive effect on
282 developmental stability. In addition, we observed that the vast majority of modifier deficiencies

283 (65 out of the 68 tested) does not affect FA on their own. Finally, the 13 deficiencies that
284 enhance *CycG*$^{\Delta P}$-induced FA represent only 4.1 % of the *Drosophila melanogaster* genome.
285 Collectively, these results indicate that under normal rearing conditions the control of growth
286 is highly robust.

287 Overexpression of *CycG*$^{\Delta P}$ using the Gal4/UAS system provides an entry point to
288 discover genes and gene networks that are essential for growth homeostasis. Unsurprisingly,
289 our results confirm that key morphogens, Dpp and Wg, are crucial for maintaining
290 developmental stability. A previous study had shown that insertional mutants of two BMP
291 pathway components, *tkv*, encoding a receptor of *dpp*, and *Mad*, encoding the principal
292 transcription factor, affect shape fluctuating asymmetry (Debat et al. 2009). Consistently, we
293 found that both a deficiency encompassing *dpp* and *dpp* mutant alleles enhance *CycG*$^{\Delta P}$-
294 induced FA, highlighting the central role of the BMP pathway in developmental stability. We
295 further show that the InR/Tor and Hippo growth pathways are essential for developmental
296 stability. In line with our findings, alternative splicing of *yki*, which encodes the transcription
297 factor Yorkie, a target of the Hippo pathway, has previously been shown to contribute to
298 developmental stability (Srivastava et al. 2020). Furthermore, Merlin that promotes assembly
299 of a functional Hippo signaling complex at the apical cell cortex has been shown to directly
300 interact with Cyclin G (Oughtred et al. 2021). With regard to the *Dilp8/Lgr3* axis (Colombani
301 et al. 2012; Garelli et al. 2012; Colombani et al. 2015; Garelli 2015), neither *Dilp8* nor *Lgr3*
302 were found in deficiencies that modify *CycG*$^{\Delta P}$-induced FA (*Df(3L)ED4685* and *Df(3L)ED4674*
303 for *Dilp8; Df(3R)BSC321* for *Lgr3*). These results are consistent with our previous findings
304 that expressing *CycG*$^{\Delta P}$ in the neuronal circuitry relaying information from the *Dilp8*
305 expression site to the brain does not modify FA. This led to conclude that *CycG*$^{\Delta P}$-induced
306 wing FA is an intrinsic response of the growing wing tissue (Dardalhon-Cuménal et al. 2018).
307 Lastly, mutants of the *Tps1* gene, which is involved in trehalose metabolism, exhibit high FA
308 that is exacerbated under dietary stress, suggesting an important role for trehalose
309 metabolism in developmental stability (Matsushita and Nishimura 2020). *Tps1* is located
310 within the *Df(2L)M24F-B* deficiency, which does not affect *CycG*$^{\Delta P}$-induced developmental
311 stability. Nevertheless, a more in-depth analysis of the interaction between *CycG* and *Tps1*,
312 particularly under dietary stress conditions, remains to be carried out.

313 Beyond its specific role, Cyclin G may be unique in that it sits at the crossroads of
314 many signalling pathways. Our previous systems biology approach has indeed shown that

315 *CycG* is linked to many genes in the wing imaginal disc (Dardalhon-Cuménal et al. 2018).
316 These new findings confirm that *CycG* may be a hub within a complex genetic network
317 important for the robustness of organ growth.

318 We have previously shown that expression of $CycG^{\Delta P}$ abolishes the strong negative
319 correlation between cell size and cell number observed in wild-type fly wings (Debat et al.
320 2011). Cyclin G may orchestrate growth homeostasis by ensuring the proper coordination of
321 growth and the cell cycle, which would be critical for developmental stability. This central role
322 may explain the spectacular effects of its deregulation on fluctuating asymmetry.

323 Some potential direct Cyclin G partners are included in the deficiencies that modify
324 $CycG^{\Delta P}$-induced FA. Strikingly, these partners belong to different gene ontology categories,
325 ranging from the aforementioned Merlin to transcription factors (*e.g.* E5), translation
326 regulators (*e.g.* Larp) and proteins involved in protein degradation (*e.g.* Cul2), reinforcing the
327 idea that Cyclin G may be involved in diverse cellular processes. Among the genes encoding
328 these potential direct partners, *larp* is the only one whose inactivation strongly reduces
329 $CycG^{\Delta P}$-induced FA, suggesting that the effect of Cyclin G on FA requires this direct
330 interaction. *Larp* encodes an evolutionarily conserved RNA-binding protein that forms a
331 complex with the Poly(A) binding protein (PABP), a translation regulator (Blagden et al. 2009;
332 Deragon and Bousquet-Antonelli 2015). In addition, Larp recognises mRNAs with a 5'
333 Terminal OligoPyrimidine (5' TOP) motif, *i.e.* mRNAs encoding proteins essential for protein
334 synthesis such as ribosomal proteins or translation factors (Cockman et al. 2020). More
335 recently, Larp has been shown to play a dual role as a translational repressor and a stabiliser
336 of 5' TOP mRNAs (20). In particular, when phosphorylated by Pink1, Larp inhibits translation
337 at the mitochondrial outer membrane suggesting that it may have an effect on the production
338 of new mitochondria (Zhang et al. 2019). Interestingly, in wing imaginal discs expressing
339 $CycG^{\Delta P}$, genes involved in translation are up-regulated and those involved in metabolism and
340 mitochondrial activity are down-regulated (Dardalhon-Cuménal et al. 2018). Taken together,
341 these data support the idea that there may be a link between developmental stability and the
342 regulation of mitochondrial activity.

343

344 **FIGURES**

345

346 **Figure 1: Secondary screen – Analysis of the 60 candidate deficiencies isolated from**

347 **the primary screen.**

348 **a –** FA of 39 deficiencies that decreased *CycG*$^{\Delta P}$-induced FA in the primary screen normalised
349 to the FA of *da-Gal4, UAS-CycG*$^{\Delta P}$ (red line). 16 of them reproduced the results of the primary
350 screen (orange).

351 **b –** FA of 21 deficiencies that enhanced *CycG*$^{\Delta P}$-induced FA in the primary screen normalised
352 to the FA of *da-Gal4, UAS-CycG*$^{\Delta P}$ (red line). 13 of them reproduced the results of the primary
353 screen (green).

354 *p<0.05, **p<0.01, ***p<0.001

355

356 **Figure 2: Secondary screen - Relationship between fluctuating asymmetry and**
357 **deficiency length, mean wing size and inter-individual variance.**

358 **a –** FA (fold change) of the 16 decreasing (D) deficiencies (orange), the 13 enhancing (E)
359 deficiencies (green) and 8 neutral deficiencies (grey) versus deficiency length. No significant
360 correlation was observed between the two parameters (Pearson coefficient, R= -0.15).

361 **b -** FA of the 16 decreasing (D) deficiencies (orange) and the 13 enhancing (E) deficiencies
362 (green) combined with *da-Gal4, UAS-CycG*$^{\Delta P}$ (filled circles) or not (empty circles) versus
363 mean wing size. Filled grey square: *+/da-Gal4, UAS-CycG*$^{\Delta P}$; empty grey square: *+/da-Gal4*.
364 A strong negative correlation was observed between these parameters (R= -0.65).

365 **c –** FA (log10) of the 16 decreasing (D) deficiencies (orange) and the 13 enhancing (E)
366 deficiencies (green) combined with *da-Gal4, UAS-CycG*$^{\Delta P}$ (filled circles) or not (empty circles)
367 versus inter-individual variance (log10). Filled grey square: *+/da-Gal4, UAS-CycG*$^{\Delta P}$; empty
368 grey square: *+/da-Gal4*. A strong positive correlation was observed between the two
369 parameters (R= +0.67).

370

371 **Figure 3: Candidate gene analyses – Genes encoding direct protein partners of**
372 **Cyclin G located in deficiencies that modify *CycG*$^{\Delta P}$-induced FA.**

373 In green, alleles that significantly increased *CycG*$^{\Delta P}$-induced FA**.** In orange, alleles that
374 significantly decreased *CycG*$^{\Delta P}$-induced FA. In light grey, positive control *(+/da-Gal4, UAS-*
375 *CycG*$^{\Delta P}$). In dark grey, alleles that did not modify *CycG*$^{\Delta P}$-induced FA. Several alleles were
376 lethal (†) when combined to *+/da-Gal4* or *+/da-Gal4, UAS-CycG*$^{\Delta P}$.

377 *p<0.05, **p<0.01, ***p<0.001

378

379 **Figure 4: Candidate gene analyses – Genes encoding members of the Hippo pathway**
380 **(a), the InR/TOR pathway (b) and the Dpp and Wg morphogens (c).**
381 In green, alleles that significantly increased *CycG*$^{\Delta P}$-induced FA**.** In grey, alleles that did not
382 modify *CycG*$^{\Delta P}$-induced FA.
383 *p<0.05, **p<0.01, ***p<0.001
384
385 **Supplementary Figure 1:**
386 **a -** Position of the 15 landmarks on the wing. Landmarks 3 and 13 (red) were used to measure
387 wing length.
388 **b –** Diagrams of primary and secondary screens.
389 *Df*: deficiency; *w*^{n}: *w*^{5905} or *w*^{6326}; *Bal*: balancer chromosome; N: neutral deficiencies; D:
390 deficiency that decreased *CycG*$^{\Delta P}$-induced fluctuating asymmetry; E: deficiency that
391 increased *CycG*$^{\Delta P}$-induced fluctuating asymmetry.
392
393 **Supplementary Figure 2: Distributions of the FA fold-changes in the primary and**
394 **secondary screens.**
395 **a –** FA fold-changes for the 452 deficiencies that produced measurable wings when combined
396 with *da-Gal4*, *UAS-CycG*$^{\Delta P}$. Orange: FA fold-changes for the 39 deficiencies that significantly
397 decreased *CycG*$^{\Delta P}$-induced FA. Green: FA of the 21 deficiencies that significantly increased
398 *CycG*$^{\Delta P}$-induced FA. Grey: FA fold-changes for deficiencies that do not significantly modify
399 *CycG*$^{\Delta P}$-induced FA. Black line: FA of the *da-Gal4*, *UAS-CycG*$^{\Delta P}$ positive control.
400 **b –** FA fold-changes for the 68 deficiencies selected for the secondary screen. Green: three
401 deficiencies showed a significantly higher FA compared to the genetic background. Grey: FA
402 fold-changes for the remaining deficiencies. Black line: FA of the *w;+/da-Gal4* genetic
403 background.
404 **c –** FA fold-changes of the 68 deficiencies selected for the secondary screen combined with
405 *w; UAS-CycG*$^{\Delta P}$*/da-Gal4*. Orange: FA fold-changes of the 16 deficiencies that significantly
406 decreased *CycG*$^{\Delta P}$-induced FA. Green: FA fold-changes for the 13 deficiencies that
407 significantly increased *CycG*$^{\Delta P}$-induced FA. Grey: FA fold-changes for deficiencies that did
408 not significantly modify *CycG*$^{\Delta P}$-induced FA. Black line: FA of the *da-Gal4*, *UAS-CycG*$^{\Delta P}$
409 positive control.
410

411 **Supplementary Figure 3: Secondary screen – Mean wing size of flies heterozygous for**
412 **the deficiencies associated with *da-Gal4* (top) or *da-Gal4, UAS-CycG$^{\Delta P}$* (down).**
413 Box-plots showing mean wing size. In grey, mean wing size of *+/da-Gal4* (**a**) or *+/da-*
414 *Gal4, UAS-CycG$^{\Delta P}$* flies. In orange, mean wing size of deficiencies that decreased *CycG$^{\Delta P}$*-
415 induced FA combined with *da-Gal4* (top) or *da-Gal4, UAS-CycG$^{\Delta P}$* (down). In green, mean
416 wing size of deficiencies that increased *CycG$^{\Delta P}$*-induced FA combined with *da-Gal4* (top) *or*
417 *da-Gal4, UAS-CycG$^{\Delta P}$* (**b**).
418 The two red lines correspond to the mean wing size of *+/da-Gal4* (1161) and *+/da-Gal4, UAS-*
419 *CycG$^{\Delta P}$* (1014) flies.
420 *p<0.05, **p<0.01, ***p<0.001

421 **Table 1: Deficiencies modifying *CycG$^{\Delta P}$*-induced FA.**

422 The fluctuating asymmetry fold-change corresponds to the ratio between fluctuating
423 asymmetry of the deficiency combined to *da-Gal4, UAS-CycG$^{\Delta P}$* and fluctuating asymmetry
424 of *da-Gal4, UAS-CycG$^{\Delta P}$*.

Chromosome arm	Deficiency name	Cytological location	Fluctuating asymmetry fold-change	Adjusted p-value
X	*Df(1)BSC530*	1A5;1B12	0.37329	4.68E-02
	Df(1)M38-C5	8B;8E	0.24024	2.86E-03
	Df(1)BSC722	10B3;10E1	0.25570	6.72E-03
	Df(1)FDD-0024486	14C4;14D1	0.12722	2.58E-06
	Df(1)BSC643	15F9;16F1	0.28609	7.33E-03
	Df(1)BSC405	16D5;16F6	0.37682	4.68E-02
	Df(1)BSC871	18D7;18F2	0.32513	2.55E-02
2L	*Df(2L)Exel7011*	22E1;22F3	3.67005	4.34E-03
	Df(2L)BSC354	26D7;26E3	4.32949	1.32E-03
	Df(2L)BSC291	27D6;27F2	2.69177	3.96E-02
	Df(2L)Exel7034	28E1;28F1	3.92670	2.69E-03
	Df(2L)ED629	29B4;29E4	6.02764	5.81E-05
	Df(2L)BSC277	34A1;34B2	0.39515	2.82E-02
	Df(2L)ED1473	39B4;40A5	3.37401	7.77E-03
	Df(2L)lt109	h35;h35	2.87894	2.34E-02
2R	*Df(2R)BSC880*	49A9;49E1	3.36810	9.85E-04
	Df(2R)ED3728	56D10;56E2	2.79286	2.50E-02
3L	*Df(3L)ED201*	61B1;61C1	9.14411	6.11E-07
	Df(3L)ED4457	67E2;68A7	3.77715	3.03E-03
	Df(3L)BSC12	69F6;70A2	7.46921	5.43E-06
	Df(3L)ED4710	74D1;75B11	5.14760	1.95E-04
	Df(3L)BSC419	78C2;78D8	0.20077	5.30E-04
3R	*Df(3R)BSC549*	83A6;83B6	0.28288	9.98E-03
	Df(3R)ED5623	87E3;88A4	0.32086	1.65E-02
	Df(3R)ED5705	88E12;89A5	0.33282	1.69E-02
	Df(3R)ED6255	97D2;97F1	0.27386	5.53E-03
	Df(3R)BSC322	98C3;98D7	0.33719	3.21E-02
	Df(3R)BSC749	100B1;100C1	0.39540	9.04E-03
	Df3R)ED6361	100C7;100E3	0.40559	1.17E-02

425

426

427 **Supplementary Table 1: Deficiencies used in this study.**

428

429 **Supplementary Table 2: Alleles used in this study to identify genes that modify *CycG*$^{\Delta P}$-**
430 **induced fluctuating asymmetry in the decreasing and enhancing deficiencies.**

431

432 **Supplementary Table 3: Secondary screen for deficiencies which modify *CycG*$^{\Delta P}$-**
433 **induced FA.**

434

435 **Supplementary Table 4: Deficiencies used in Takahashi, Okada, Teramura, et al. (2011)**
436 **that are shared or overlap with those used in the secondary screen.**

437

Data availability statement

The authors confirm that all the data necessary to verify the conclusions of the article are included in the text, figures and tables. Strains are available upon request. Raw data are deposited on Zenodo (DOI 10.5281/zenodo.17416429).

Acknowledgments

The authors would like to thank all the members of the Heterochromatin, Cell Fate and Exposome team for their valuable advice and productive discussions. They would also like to thank Dr. Y. Bellaïche for providing the *Akt1[1]* mutant, and the Bloomington Stock Center for mutant and deficiency strains.

Study funding

This study was funded by ongoing support from the Centre National de la Recherche Scientifique (CNRS) and Sorbonne Université (SU).

REFERENCES

Berman AJ et al. 2021. Controversies around the function of LARP1. RNA Biol. 18(2):207–217. https://doi.org/10.1080/15476286.2020.1733787

Bettencourt-Dias M et al. 2004. Genome-wide survey of protein kinases required for cell cycle progression. Nature. 432(7020):980–7. https://doi.org/10.1038/nature03160

Blagden SP et al. 2009. *Drosophila* Larp associates with poly(A)-binding protein and is required for male fertility and syncytial embryo development. Dev Biol. 334(1):186–197. https://doi.org/10.1016/j.ydbio.2009.07.016

Breuker CJ, Patterson JS, Klingenberg CP. 2006. A single basis for developmental buffering of *Drosophila* wing shape. PLoS ONE. 1:e7. https://doi.org/10.1371/journal.pone.0000007

Carvalhal S et al. 2015. The nucleoporin ALADIN regulates Aurora A localization to ensure robust mitotic spindle formation Zheng Y, editor. Mol Biol Cell. 26(19):3424–3438. https://doi.org/10.1091/mbc.E15-02-0113

467 Cockman E, Anderson P, Ivanov P. 2020. TOP mRNPs: Molecular Mechanisms and
468 Principles of Regulation. Biomolecules. 10(7):969. https://doi.org/10.3390/biom10070969

469 Colombani J et al. 2015. *Drosophila* Lgr3 Couples Organ Growth with Maturation and
470 Ensures Developmental Stability. Curr Biol. 25:2723–2729.
471 https://doi.org/10.1016/j.cub.2015.09.020

472 Colombani J, Andersen DS, Léopold P. 2012. Secreted peptide Dilp8 coordinates
473 *Drosophila* tissue growth with developmental timing. Science. 336(6081):582–5.
474 https://doi.org/10.1126/science.1216689

475 Cook RK et al. 2012. The generation of chromosomal deletions to provide extensive
476 coverage and subdivision of the *Drosophila melanogaster* genome. Genome Biol.
477 13(3):R21. https://doi.org/10.1186/gb-2012-13-3-r21

478 Dalton D, Chadwick R, McGinnis W. 1989. Expression and embryonic function of empty
479 spiracles: a *Drosophila* homeo box gene with two patterning functions on the anterior-
480 posterior axis of the embryo. Genes Dev. 3(12a):1940–1956.
481 https://doi.org/10.1101/gad.3.12a.1940

482 Dardalhon-Cuménal D et al. 2018. Cyclin G and the Polycomb Repressive complexes
483 PRC1 and PR-DUB cooperate for developmental stability. PLoS Genet. 14(7):e1007498.
484 https://doi.org/10.1371/journal.pgen.1007498

485 Debat V et al. 2011. Developmental Stability: A Major Role for Cyclin G in *Drosophila*
486 *melanogaster*. PLoS Genet. 7(10):e1002314. https://doi.org/10.1371/journal.pgen.1002314

487 Debat V, David JR. 2002. Analysing phenotypic variation: when old-fashioned means up-to-
488 date. J Biosci. 27(3):191–193.

489 Debat V, Debelle A, Dworkin I. 2009. Plasticity, canalization and developmental stability of
490 the drosophila wing: joint effect of mutations and of developmental temperature. Evolution.
491 63-11:2864–2876. https://doi.org/doi:10.1111/j.1558-5646.2009.00774.x

492 Debat V, Peronnet F. 2013. Asymmetric flies: The control of developmental noise in
493 *Drosophila*. Fly Austin. 7(2):1–8. https://doi.org/10.4161/fly.23558

494 Deragon J, Bousquet-Antonelli C. 2015. The role of LARP1 in translation and beyond.
495 WIREs RNA. 6(4):399–417. https://doi.org/10.1002/wrna.1282

496 Fischer P, Preiss A, Nagel AC. 2016. A triangular connection between Cyclin G, PP2A and
497 Akt1 in the regulation of growth and metabolism in *Drosophila*. Fly (Austin). 1–8.
498 https://doi.org/10.1080/19336934.2016.1162362

499 Garelli A et al. 2012. Imaginal discs secrete insulin-like peptide 8 to mediate plasticity of
500 growth and maturation. Science. 336(6081):579–82.
501 https://doi.org/10.1126/science.1216735

502 Garelli A. 2015. Dilp8 requires the neuronal relaxin receptor Lgr3 to couple growth to
503 developmental timing. Nat Commun. 6:8732. https://doi.org/10.1038

504 Gomez FH, Norry FM. 2012. Is the number of possible QTL for asymmetry phenotypes
505 dependent on thermal stress? J Therm Biol. 37(1):1–5.
506 https://doi.org/DOI%252010.1016/j.jtherbio.2011.10.001

507 Grewal SS. 2009. Insulin/TOR signaling in growth and homeostasis: a view from the fly
508 world. Int J Biochem Cell Biol. 41(5):1006–10. https://doi.org/10.1016/j.biocel.2008.10.010

509 Hoskins RA et al. 2001. Single Nucleotide Polymorphism Markers for Genetic Mapping in
510 *Drosophila melanogaster*. Genome Res. 11(6):1100–1113.
511 https://doi.org/10.1101/gr.178001

512 Klingenberg CP. 2019. Phenotypic Plasticity, Developmental Instability, and Robustness:
513 The Concepts and How They Are Connected. Front Ecol Evol. 7:56.
514 https://doi.org/10.3389/fevo.2019.00056

515 Leamy L et al. 2015. The Genetic Architecture of Fluctuating Asymmetry of Mandible Size
516 and Shape in a Population of Mice: Another Look. Symmetry. 7(1):146–163.
517 https://doi.org/10.3390/sym7010146

518 Marygold SJ, Attrill H, Lasko P. 2017. The translation factors of *Drosophila melanogaster*.
519 Fly Austin. 11(1):65–74. https://doi.org/10.1080/19336934.2016.1220464

520 Matsushita R, Nishimura T. 2020. Trehalose metabolism confers developmental robustness
521 and stability in Drosophila by regulating glucose homeostasis. Commun Biol. 3(1):170.
522 https://doi.org/10.1038/s42003-020-0889-1

523 Neto-Silva RM, Wells BS, Johnston LA. 2009. Mechanisms of growth and homeostasis in
524 the *Drosophila* wing. Annu Rev Cell Dev Biol. 25:197–220.
525 https://doi.org/10.1146/annurev.cellbio.24.110707.175242

526 Oughtred R et al. 2021. The BIOGRID database: A comprehensive biomedical resource of
527 curated protein, genetic, and chemical interactions. Protein Sci. 30(1):187–200.
528 https://doi.org/10.1002/pro.3978

529 Palmer RA. 1994. Fluctuating asymmetry analysis: a primer. In: Developmental Instability:
530 Its Origins and Evolutionary Implications. T. A. Markow. Netherlands, Kluwer Academic
531 Publishers; p 335–364

532 Palmer, A. R., Strobeck, C. 2003. Fluctuating asymmetry analyses revisited. In:
533 Developmental Instability: Causes and Consequences. p 279–319.

534 Roote J, Russell S. 2012. Toward a complete *Drosophila* deficiency kit. Genome Biol.
535 13(3):149. https://doi.org/10.1186/gb-2012-13-3-149

536 Ryder E et al. 2004. The DrosDel collection: a set of P-element insertions for generating
537 custom chromosomal aberrations in *Drosophila melanogaster*. Genetics. 167(2):797–813.
538 https://doi.org/10.1534/genetics.104.026658

539 Srivastava D et al. 2020. Modulation of *Yorkie* activity by alternative splicing is required for
540 developmental stability. EMBO J. [published online ahead of print].
541 https://doi.org/10.15252/embj.2020104895

542 Tabata T, Takei Y. 2004. Morphogens, their identification and regulation. Development.
543 131(4):703–712. https://doi.org/10.1242/dev.01043

544 Takahashi KH et al. 2010. Effects of small *Hsp* genes on developmental stability and
545 microenvironmental canalization. BMC Evol Biol. 10:284. https://doi.org/10.1186/1471-
546 2148-10-284

547 Takahashi KH, Okada Y, Teramura K. 2011. Genome-Wide Deficiency Mapping of the
548 Regions Responsible for Temporal Canalization of the Developmental Processes of
549 *Drosophila melanogaster*. J Hered. 102(4):448–57. https://doi.org/10.1093/jhered/esr026

550 Takahashi KH, Okada Y, Teramura K, Tsujino M. 2011. Deficiency mapping of the genomic
551 regions associated with effects on developmental stability in *Drosophila melanogaster*.
552 Evolution. 65:3565–3577

553 Zhang Y et al. 2019. PINK1 Inhibits Local Protein Synthesis to Limit Transmission of
554 Deleterious Mitochondrial DNA Mutations. Mol Cell. 73(6):1127-1137.e5.
555 https://doi.org/10.1016/j.molcel.2019.01.013

Figure 1

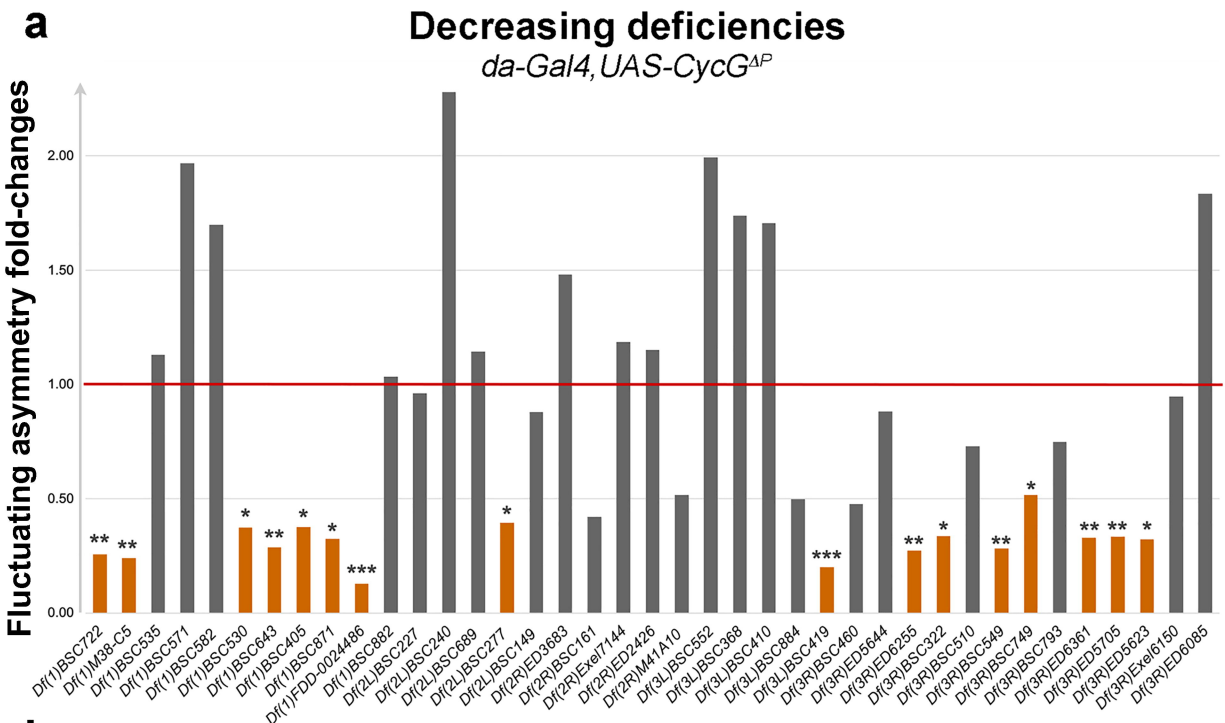
a
Decreasing deficiencies
da-Gal4, UAS-CycG$^{\Delta P}$
Fluctuating asymmetry fold-changes
0.00
0.50
1.00
1.50
2.00
Df(1)BSC722
Df(1)M38-C5
Df(1)BSC535
Df(1)BSC571
Df(1)BSC582
Df(1)BSC530
Df(1)BSC643
Df(1)BSC405
Df(1)BSC871
Df(1)FDD-0024486
Df(1)BSC882
Df(2L)BSC227
Df(2L)BSC240
Df(2L)BSC689
Df(2L)BSC277
Df(2L)BSC149
Df(2R)ED3683
Df(2R)BSC161
Df(2R)Exel7144
Df(2R)ED2426
Df(2R)M41A10
Df(3L)BSC552
Df(3L)BSC368
Df(3L)BSC410
Df(3L)BSC884
Df(3L)BSC419
Df(3R)BSC460
Df(3R)ED5644
Df(3R)ED6255
Df(3R)BSC322
Df(3R)BSC510
Df(3R)BSC549
Df(3R)BSC749
Df(3R)BSC793
Df(3R)ED6361
Df(3R)ED5705
Df(3R)ED5623
Df(3R)Exel6150
Df(3R)ED6085

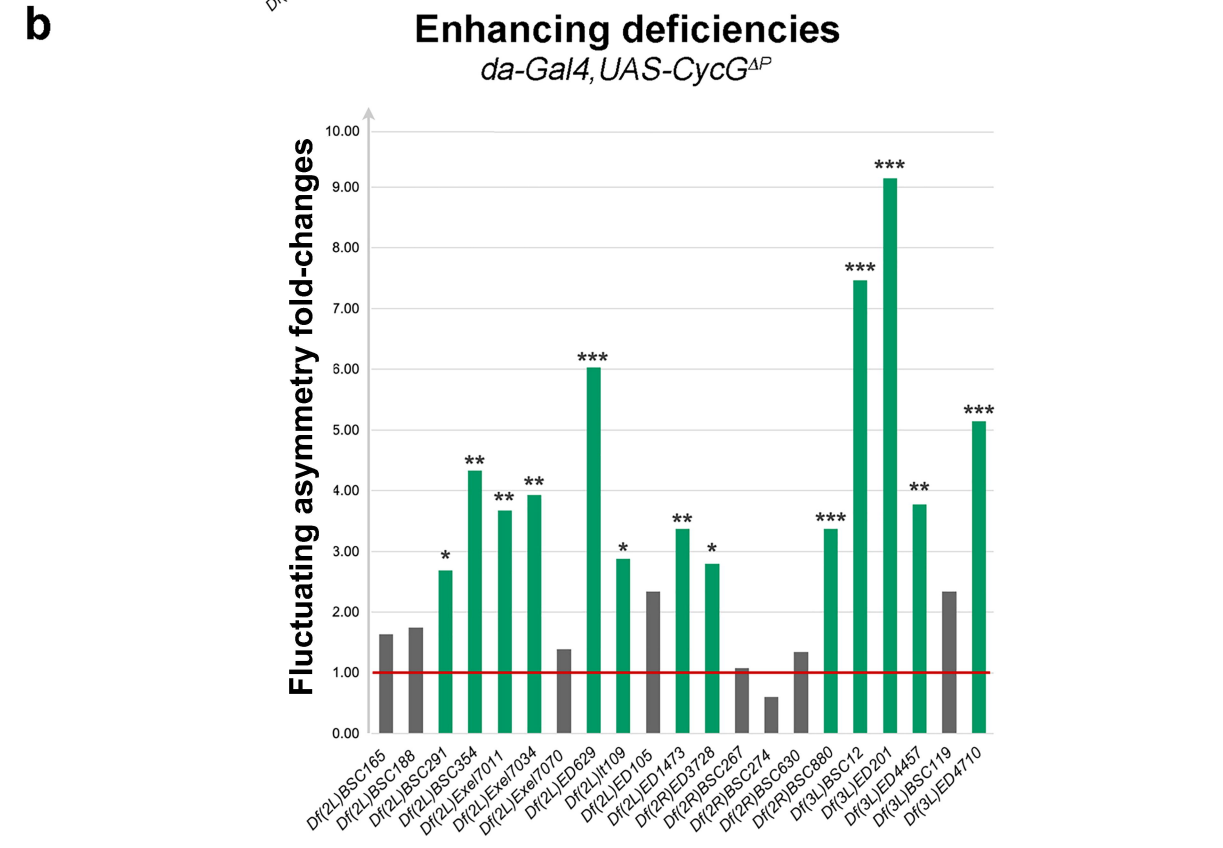
b
Enhancing deficiencies
da-Gal4, UAS-CycG$^{\Delta P}$
Fluctuating asymmetry fold-changes
0.00
1.00
2.00
3.00
4.00
5.00
6.00
7.00
8.00
9.00
10.00
Df(2L)BSC165
Df(2L)BSC188
Df(2L)BSC291
Df(2L)BSC354
Df(2L)Exel7011
Df(2L)Exel7034
Df(2L)Exel7070
Df(2L)ED629
Df(2L)lft109
Df(2L)ED105
Df(2L)ED1473
Df(2R)ED3728
Df(2R)BSC267
Df(2R)BSC274
Df(2R)BSC630
Df(2R)BSC880
Df(3L)BSC12
Df(3L)ED201
Df(3L)ED4457
Df(3L)BSC119
Df(3L)ED4710

Figure 2

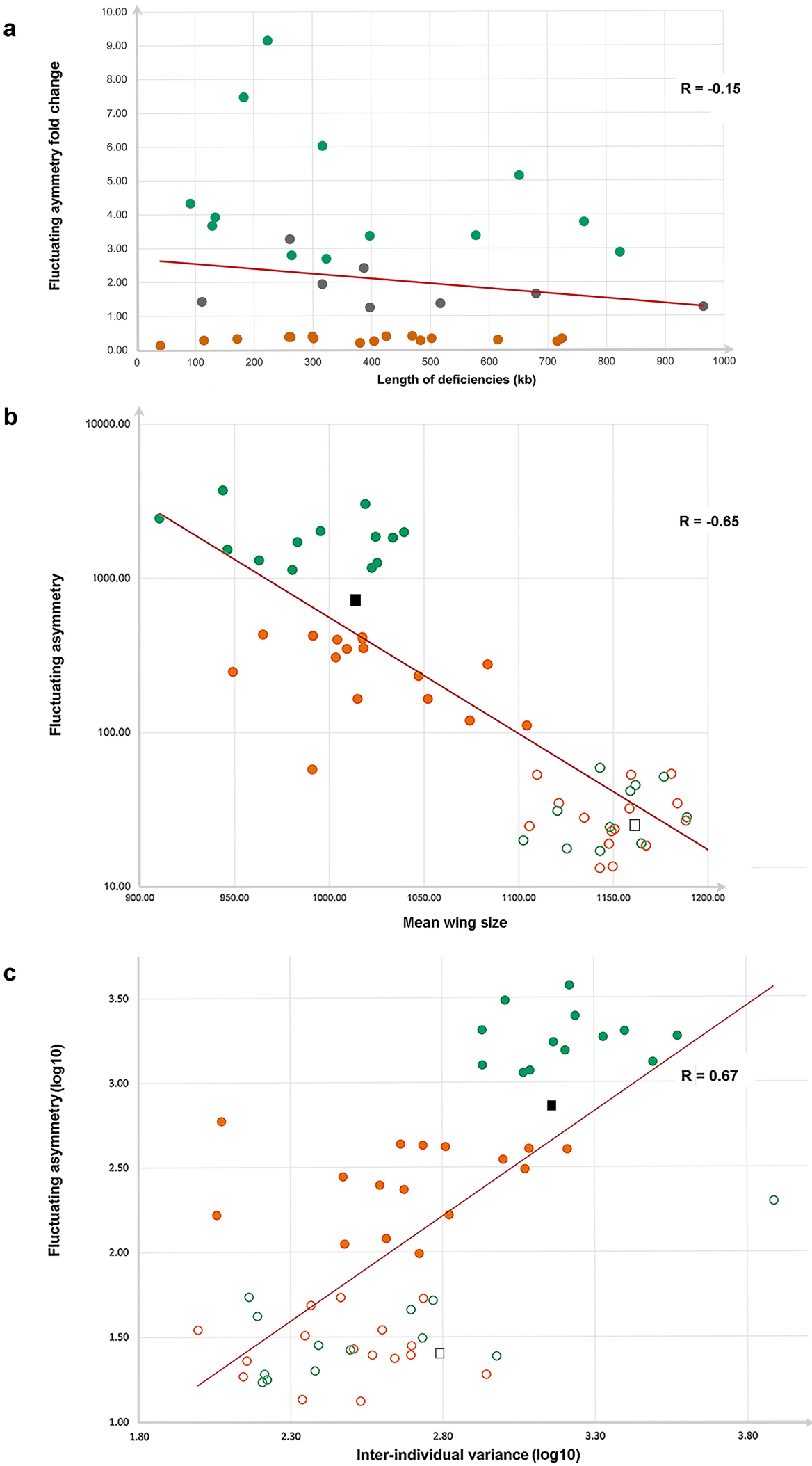
a
Fluctuating aymmetry fold change
10.00
9.00
8.00
7.00
6.00
5.00
4.00
3.00
2.00
1.00
0.00
0
100
200
300
400
500
600
700
800
900
1000
Length of deficiencies (kb)
R = -0.15
b
Fluctuating asymmetry
10000.00
1000.00
100.00
10.00
900.00
950.00
1000.00
1050.00
1100.00
1150.00
1200.00
Mean wing size
R = -0.65
c
Fluctuating asymmetry (log10)
3.50
3.00
2.50
2.00
1.50
1.00
1.80
2.30
2.80
3.30
3.80
Inter-individual variance (log10)
R = 0.67

Figure 3

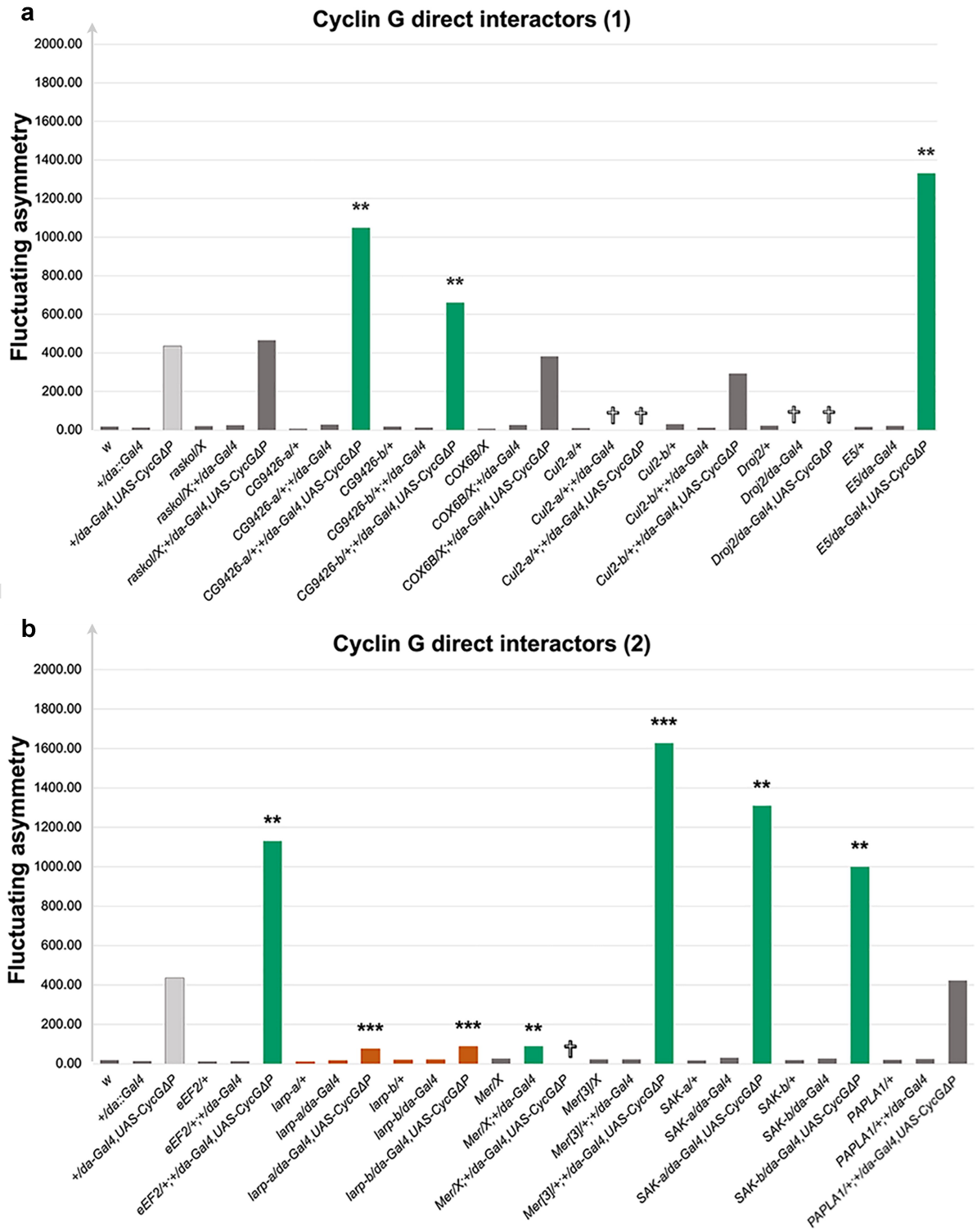
a
Cyclin G direct interactors (1)
Fluctuating asymmetry
2000.00
1800.00
1600.00
1400.00
1200.00
1000.00
800.00
600.00
400.00
200.00
0.00
**
**
**
†
†
†
†
w
+/da::Gal4
+/da-Gal4,UAS-CycGΔP
raskol/X
raskol/X;+/da-Gal4
raskol/X;+/da-Gal4,UAS-CycGΔP
CG9426-a/+
CG9426-a/+;+/da-Gal4
CG9426-a/+;+/da-Gal4,UAS-CycGΔP
CG9426-b/+
CG9426-b/+;+/da-Gal4
CG9426-b/+;+/da-Gal4,UAS-CycGΔP
COX6B/X
COX6B/X;+/da-Gal4
COX6B/X;+/da-Gal4,UAS-CycGΔP
Cul2-a/+
Cul2-a/+;+/da-Gal4
Cul2-a/+;+/da-Gal4,UAS-CycGΔP
Cul2-b/+
Cul2-b/+;+/da-Gal4
Cul2-b/+;+/da-Gal4,UAS-CycGΔP
Droj2/+
Droj2/da-Gal4
Droj2/da-Gal4,UAS-CycGΔP
E5/+
E5/da-Gal4
E5/da-Gal4,UAS-CycGΔP
b
Cyclin G direct interactors (2)
Fluctuating asymmetry
2000.00
1800.00
1600.00
1400.00
1200.00
1000.00
800.00
600.00
400.00
200.00
0.00
**
***
***
**
†
***
**
**
w
+/da::Gal4
+/da-Gal4,UAS-CycGΔP
eEF2/+
eEF2/+;+/da-Gal4
eEF2/+;+/da-Gal4,UAS-CycGΔP
larp-a/+
larp-a/da-Gal4
larp-a/da-Gal4,UAS-CycGΔP
larp-b/+
larp-b/da-Gal4
larp-b/da-Gal4,UAS-CycGΔP
Mer/X
Mer/X;+/da-Gal4
Mer/X;+/da-Gal4,UAS-CycGΔP
Mer[3]/X
Mer[3]/+;+/da-Gal4
Mer[3]/+;+/da-Gal4,UAS-CycGΔP
SAK-a/+
SAK-a/da-Gal4
SAK-a/da-Gal4,UAS-CycGΔP
SAK-b/+
SAK-b/da-Gal4
SAK-b/da-Gal4,UAS-CycGΔP
PAPLA1/+
PAPLA1/+;+/da-Gal4
PAPLA1/+;+/da-Gal4,UAS-CycGΔP

Figure 4

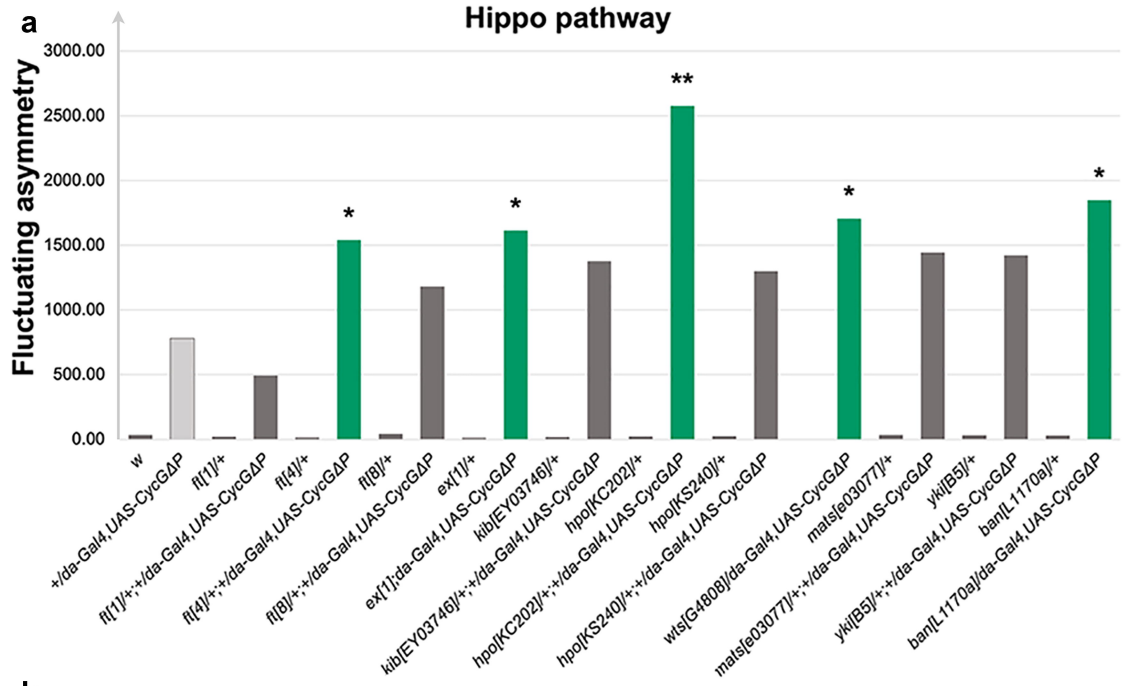
a
Hippo pathway
Fluctuating asymmetry
3000.00
2500.00
2000.00
1500.00
1000.00
500.00
0.00
w
+/da-Gal4,UAS-CycGΔP
ft[1]/+
ft[1]/+;+/da-Gal4,UAS-CycGΔP
ft[4]/+
ft[4]/+;+/da-Gal4,UAS-CycGΔP
ft[8]/+
ft[8]/+;+/da-Gal4,UAS-CycGΔP
ex[1]/+
ex[1];da-Gal4,UAS-CycGΔP
kib[EY03746]/+
kib[EY03746]/+;+/da-Gal4,UAS-CycGΔP
hpo[KC202]/+
hpo[KC202]/+;+/da-Gal4,UAS-CycGΔP
hpo[KS240]/+
hpo[KS240]/+;+/da-Gal4,UAS-CycGΔP
wts[G4808]/da-Gal4,UAS-CycGΔP
mats[e03077]/+
mats[e03077]/+;+/da-Gal4,UAS-CycGΔP
yki[B5]/+
yki[B5]/+;+/da-Gal4,UAS-CycGΔP
ban[L1170a]/+
ban[L1170a]/da-Gal4,UAS-CycGΔP

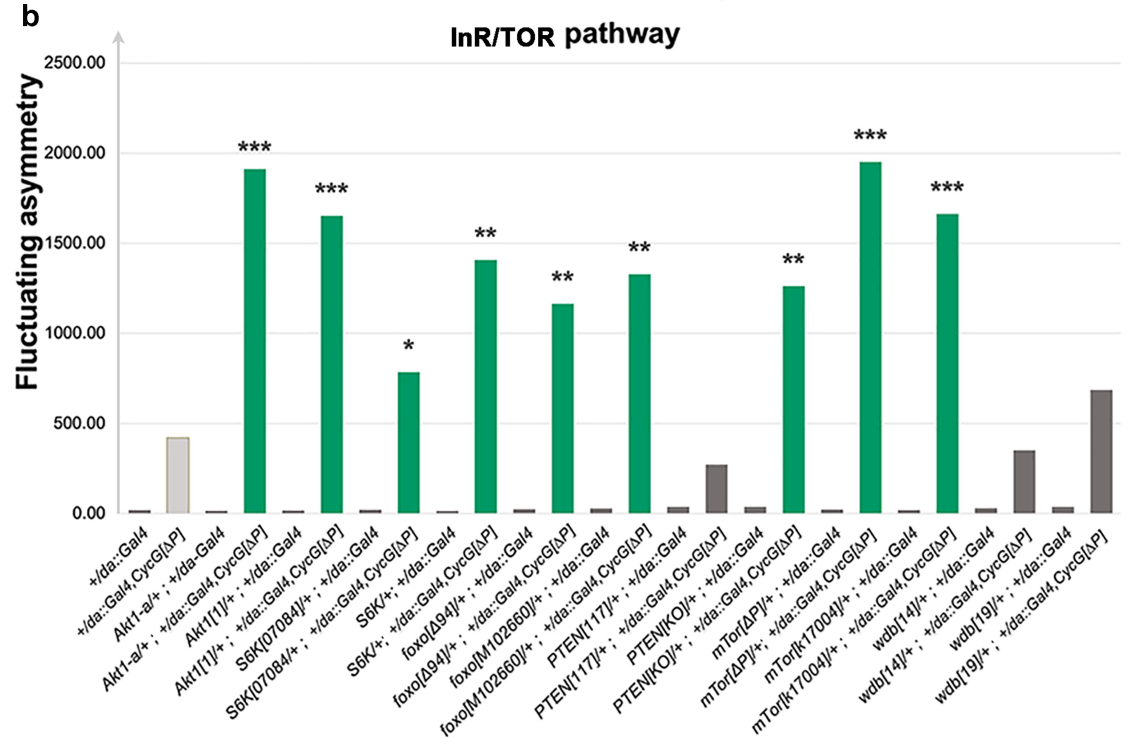
b
InR/TOR pathway
Fluctuating asymmetry
2500.00
2000.00
1500.00
1000.00
500.00
0.00
+/da::Gal4
+/da::Gal4,CycG[ΔP]
Akt1-a/+ ; +/da-Gal4
Akt1-a/+ ; +/da::Gal4,CycG[ΔP]
Akt1-a/+ ; +/da::Gal4
Akt1[1]/+ ; +/da::Gal4,CycG[ΔP]
Akt1[1]/+ ; +/da::Gal4
Akt1[1]/+ ; +/da::Gal4,CycG[ΔP]
S6K[07084]/+ ; +/da::Gal4
S6K[07084]/+ ; +/da::Gal4,CycG[ΔP]
S6K/+ ; +/da::Gal4
S6K/+ ; +/da::Gal4,CycG[ΔP]
foxo[Δ94]/+ ; +/da::Gal4
foxo[Δ94]/+ ; +/da::Gal4,CycG[ΔP]
foxo[M102660]/+ ; +/da::Gal4
foxo[M102660]/+ ; +/da::Gal4,CycG[ΔP]
PTEN[117]/+ ; +/da::Gal4
PTEN[117]/+ ; +/da::Gal4,CycG[ΔP]
PTEN[KO]/+ ; +/da::Gal4
PTEN[KO]/+ ; +/da::Gal4,CycG[ΔP]
mTor[ΔP]/+ ; +/da::Gal4
mTor[ΔP]/+ ; +/da::Gal4,CycG[ΔP]
mTor[k17004]/+ ; +/da::Gal4
mTor[k17004]/+ ; +/da::Gal4,CycG[ΔP]
wdb[14]/+ ; +/da::Gal4
wdb[14]/+ ; +/da::Gal4,CycG[ΔP]
wdb[19]/+ ; +/da::Gal4
wdb[19]/+ ; +/da::Gal4,CycG[ΔP]

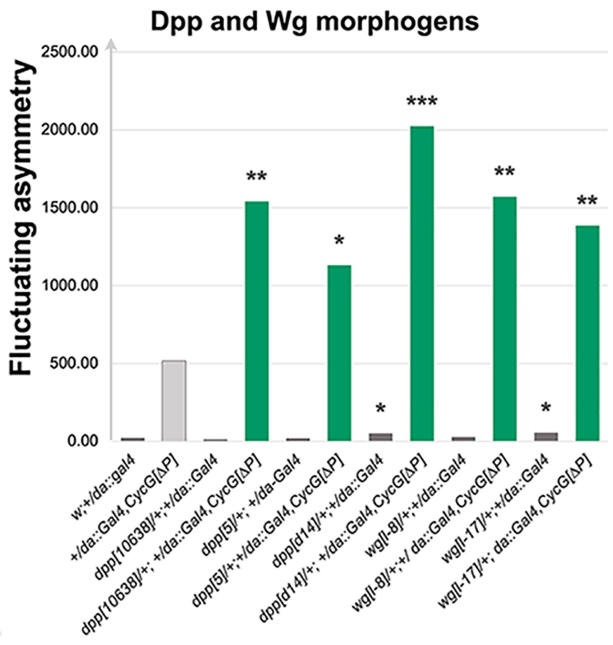
c
Dpp and Wg morphogens
Fluctuating asymmetry
2500.00
2000.00
1500.00
1000.00
500.00
0.00
w;+/da::gal4
+/da::Gal4,CycG[ΔP]
dpp[10638]/+;+/da::Gal4
dpp[10638]/+;+/da::Gal4,CycG[ΔP]
dpp[5]/+;+/da-Gal4
dpp[5]/+;+/da::Gal4,CycG[ΔP]
dpp[d14]/+;+/da::Gal4
dpp[d14]/+;+/da::Gal4,CycG[ΔP]
wg[l-8]/+;+/da::Gal4
wg[l-8]/+;+/ da::Gal4,CycG[ΔP]
wg[l-17]/+;+/da::Gal4
wg[l-17]/+; da::Gal4,CycG[ΔP]